BioStudio -T

Cell Observation Device

Nikon's BioStudio-T was designed specifically for research applications in the field of regenerative medicine and stem cell biology and for use in cell manufacturing facilities. A compact live-cell imaging microscope, the BioStudio-T fits inside most incubators and is compatible with a variety of sterilization methods including vaporized H_2O_2. The fixed-stage, scanning lens system also provides a superior solution for long-term time lapse imaging and large image acquisition.

For more information on the BioStudio-T,
visit www.microscope.healthcare.nikon.com/biostudio-t

nikon-instruments-inc- nikoninstrumentsinc nikoninst nikoninstruments
Nikon Instruments Inc. | www.microscope.healthcare.nikon.com | nikoninstruments@nikon.net

STEM CELLS®

TISSUE-SPECIFIC STEM CELLS

Hypoxia Differentially Modulates the Genomic Stability of Clinical-Grade ADSCs and BM-MSCs in Long-Term Culture

NICOLAS BIGOT,[a,b,c] AUDREY MOUCHE,[a,b,c] MILENA PRETI,[d,e,f] SÉVERINE LOISEL,[a,b,c] MARIE-LAURE RENOUD,[d,e,f] RÉMY LE GUÉVEL,[b,g] LUC SENSEBÉ,[d,e,f] KARIN TARTE,[a,b,c,h] RÉMY PEDEUX[a,b,c]

Key Words. Adipose-derived stromal cell • Bone marrow-mesenchymal stromal/stem cell • Hypoxia • DNA repair • Long-term culture

[a]INSERM U917, Microenvironnement et Cancer, Rennes, France; [b]Université de Rennes 1, Rennes, France; [c]Etablissement Français du Sang Bretagne, Rennes, France; [d]Etablissement Français du Sang Pyrénées Méditerranée, Toulouse, France; [e]Université Paul Sabatier, Toulouse, France; [f]UMR5273-INSERM U1031, Toulouse, France; [g]ImPACcell, SFR Biosit, Université de Rennes 1, Rennes, France; [h]Service ITeCH, CHU Pontchaillou, Rennes, France

Correspondence: Rémy Pedeux, Ph.D., Faculté de Médecine de Rennes, Bâtiment 2, Pièce 117, 2, Avenue du Pr Léon Bernard, 35043 Rennes, France. Telephone: 33-0-2-23-23-47-02; Fax: 33-0-2-23-23-49-58; e-mail: remy.pedeux@univ-rennes1

Received April 2, 2015; accepted for publication August 2, 2015; first published online in STEM CELLS *EXPRESS* September 30, 2015.

1066-5099/2015/$30.00/0

http://dx.doi.org/10.1002/stem.2195

ABSTRACT

Long-term cultures under hypoxic conditions have been demonstrated to maintain the phenotype of mesenchymal stromal/stem cells (MSCs) and to prevent the emergence of senescence. According to several studies, hypoxia has frequently been reported to drive genomic instability in cancer cells and in MSCs by hindering the DNA damage response and DNA repair. Thus, we evaluated the occurrence of DNA damage and repair events during the ex vivo expansion of clinical-grade adipose-derived stromal cells (ADSCs) and bone marrow (BM)-derived MSCs cultured with platelet lysate under 21% (normoxia) or 1% (hypoxia) O_2 conditions. Hypoxia did not impair cell survival after DNA damage, regardless of MSC origin. However, ADSCs, unlike BM-MSCs, displayed altered γH2AX signaling and increased ubiquitylated γH2AX levels under hypoxic conditions, indicating an impaired resolution of DNA damage-induced foci. Moreover, hypoxia specifically promoted BM-MSC DNA integrity, with increased *Ku80, TP53BP1, BRCA1,* and *RAD51* expression levels and more efficient nonhomologous end joining and homologous recombination repair. We further observed that hypoxia favored mtDNA stability and maintenance of differentiation potential after genotoxic stress. We conclude that long-term cultures under 1% O_2 were more suitable for BM-MSCs as suggested by improved genomic stability compared with ADSCs. STEM CELLS *2015;33:3608–3620*

SIGNIFICANCE STATEMENT

Human mesenchymal stem cells (MSCs) feature differentiation capacities, immunomodulatory properties and therefore represent a great potential for medicine. In vitro culture allows their amplification for suitable clinical uses. Hypoxia seems relevant for the prevention of senescence and loss of MSC features. However, hypoxia is shown to promote cancer or DNA damage response (DDR) and repair failures. We demonstrate that long-term culture of MSCs with platelet lysate in hypoxia does not necessarily inhibit DDR and DNA repair. Here, bone marrow-MSCs conserved or rather improved their DDR and DNA repair (NHEJ, HR), mtDNA stability in hypoxia compared to adipose-derived stem cells. Moreover, the ubiquitylation status of gH2AX between BM-MSCs and ADSCs might be responsible for changes in their DNA repair activities. Appropriate oxygen tension seems crucial to preserve the MSCs genomic stability according to their origins.

INTRODUCTION

Human mesenchymal stromal/stem cells (MSCs) are nonhematopoietic progenitors that are characterized by their differentiation capacities [1], their immunomodulatory properties [2, 3], and their trophic functions. Furthermore, MSCs represent a vast potential for clinical purposes and are used for treating degenerative and immune disorders, including autoimmune and graft-versus-host diseases [4].

MSCs can be isolated from various sources including bone marrow (BM) and adipose tissue in adults or the umbilical cord in postnatal tissues. However, MSCs remain scarce, and the production yield generally declines with donor age. Because therapy protocols require approximately 10–100 million MSCs, ex vivo expansion is needed to obtain the required amount of cells. However, the in vitro expansion of MSCs presents some major challenges [5, 6]. Cultures are usually performed under 21% O_2, a condition that does

not reproduce the physiological context of the tissue niches and that promotes replicative stress, leading to genetic instability and senescence [7–9] as well as a loss of viability or stem cell features [8, 10].

Replicative stress, cell metabolism byproducts continuously expose cells to DNA damages. Moreover, ionizing radiations or chemotherapy drugs are exogenous agents that generate DNA breaks as well. DNA double-strand breaks (DSBs) are the most toxic lesions, they are usually sensed by the ATM kinase which drives the ATM-p53 DNA damage response (DDR) promoting cell cycle arrest and DNA repair [11]. Thus, ATM phosphorylates the H2AX variant (γH2AX) and 53BP1, to promote their rapid focal accumulations to DNA breaks. These events are crucial for the later recruitments of DNA repair proteins involved in homologous recombination (HR), like BRCA1 or Rad51 or in nonhomologous end joining (NHEJ), like Artemis or Ku80 [12, 13].

Cultures under low oxygen tension (0.2%–5% O_2) have been used to mimic the niche microenvironment and to maintain MSC characteristics. Hypoxia has been frequently found to delay the emergence of senescence in MSCs [14, 15]. Nevertheless, studies regarding genomic stability under low oxygen tension have led to conflicting results. In particular, hypoxia has been shown to reduce the occurrence of exogenous DSBs and chromosomal abnormalities or to enhance DNA repair in various models of stem cells [16, 17]. However, other studies have demonstrated that low oxygen levels lead to decreased expression of proteins involved in DNA repair processes, such as BRCA1 or Rad51 [18–20].

Thus far, the genomic stability of MSCs has only been evaluated under classical culture conditions using serum from animal origins. Here, we aimed to assess whether clinical-grade adipose-derived stromal cells (ADSCs) and BM-MSCs cultured with human platelet lysate (PL) could manifest appropriate DDRs and repair during their expansion under normoxic or hypoxic conditions and maintain genomic stability. Although hypoxia reduced p53 activation at early passages in BM-MSCs following doxorubicin treatment, efficient recognition of DNA damage was observed. Moreover, DNA repair protein expression, HR, and NHEJ activities increased in BM-MSCs cultured under hypoxic conditions, but not in ADSCs. Thus, hypoxia not only promoted processes to ensure the genomic stability of BM-MSCs but also provided stability for the mitochondrial DNA (mtDNA) and maintained the differentiation potential of MSCs recovering from genotoxic stress.

Materials and Methods

MSC Isolation and Long-Term Culture Conditions

Human ADSCs were obtained from the stromal vascular fraction (SVF) of adipose tissue as described previously [21]. In brief, abdominal dermolipectomies were obtained from three female young adults (36, 22, and 31 years old with body mass indexes of 27.08, 27.7, and 27.4, respectively) undergoing reconstructive surgery after weight loss (Plastic surgery department, University hospital, Toulouse, France). Cells from the SVF were seeded at 1,000 cells per square centimeter in αMEM supplemented with human PL (2%), heparin (1 U/ml), penicillin (100 U/ml), and streptomycin (100 μg/ml; Life Technologies, St Aubin, France) at 37°C under 21% O_2 (normoxia) or 1% O_2 (hypoxia). The ADSC primary lines were established from each donor after the generation of colony-forming unit-fibroblasts (CFU-F), attesting the formation of mesenchymal stem cells. Then, ADSCs were split and expanded either under normoxic or hypoxic conditions. The cells were cultured with αMEM supplemented with PL (2%), heparin (1 U/ml), penicillin (100 U/ml), and streptomycin (100 μg/ml). The media were changed every 3 days. The cells were passaged at near confluence and seeded at 2,000 cells per square centimeter. ADSCs from the three different donors at the end of P2 and P5 were used in the experiments. The medium used in the experiments was identical to that used for cell expansion. ADSCs were immunophenotyped at the end of P1, 4, and 10 (Supporting Information Fig. S1).

BM was harvested from three male donors (55, 21, and 23 years old) undergoing allogeneic transplantation (Hematologic Department, University Hospital, Toulouse, France). Nucleated BM cells were plated at 10^5 cells per square centimeter in a two-level CellSTACK cell culture chamber containing αMEM supplemented with human PL (8%), heparin (1 U/ml), penicillin (100 U/ml), and streptomycin (100 μg/ml; P0). The entire medium was renewed every 3 days until the cells reached confluence (the end of P0). As for ADSCs, the BM-MSCs from each donor were segregated in two groups. One group was cultured under normoxic conditions and the other group in hypoxic conditions. The cells were plated at 2,000 cells per square centimeter and expanded with αMEM containing PL (8%), heparin, penicillin, and streptomycin. The medium used for BM-MSCs during the experiments consisted of αMEM containing PL (4%), heparin, penicillin, and streptomycin. The BM-MSCs were immunophenotyped at the end of P1, 4, and 7 (Supporting Information Fig. S1).

Cells were detached and immunophenotyped, respectively, at the end of P1, 4, and 10 for ADSCs and end of P1, 4, and 7 for BM-MSCs (Supporting Information Fig. S1). Then, batches of cells were frozen and stocked. For experiments, cells were thawed and reseeded. Therefore, the experiments were conducted at P2 or P5).

All tissues were obtained following the signature of a nonobjection certificate in accordance with French bioethics law no. 2004-800 of August 6, 2004. Mesenchymal stem/stromal cells were cultured according to the GMP processes for clinical purposes.

Immunofluorescence Staining and ArrayScan Analysis

MSCs were seeded in 96-well black plates (Nunc provided by Dutscher, Brumath, France; 12,000 cells/well). The cells were washed three times with 1 × PBS and fixed in an ice-cold ethanol/acetic acid solution (95%/5%) for 5 minutes. Then, the cells were washed three times for 2 minutes with 1 × PBS-Tween 20 (0.2%) and blocked for 45 minutes with 1 × PBS-chicken serum (10%; Sigma-Aldrich, St Quentin Fallavier, France). The cells were incubated for 1 hour with primary antibodies diluted in 1 × PBS-chicken serum (10%) and Hoechst dye (2.5 ng/ml; 33342, Sigma-Aldrich). The cells were washed three times for 2 minutes with 1 × PBS-Tween 20 (0.2%) and incubated for 1 hour with secondary antibody (Alexa Fluor 647-conjugated AffiniPure F(ab')$_2$, Jackson ImmunoResearch Laboratories, West Grove, PA). Eventually, the cells were submitted to three final washing steps with PBS-Tween 20 and covered with 100 μl of MilliQ water. The primary antibodies used targeted γH2AX (Cell Signaling, provided by Ozyme, St Quentin en Yvelines, France) and 53BP1 (Santa Cruz Biotechnology, Heidelberg, Germany) (Supporting Information Table S4 for antibodies detailed references). The plates were kept in the dark at 4°C until analysis.

Images were acquired on an ArrayScan VTI high content screening reader with a ×20 lens (Thermo Scientific, Villebon sur Yvette, France). The images were analyzed using Cell Profiler software (http://www.cellprofiler.org, Broad Institute). In brief, spots corresponding to focal accumulations of targeted proteins were detected before or after genotoxic stress. Settings were chosen for each tested antibody to optimize the differences between control and treated cells. For all analyses, raw data files were obtained, and the total amount of Hoechst fluorescence, the total amount of relevant antibody fluorescence, and the number of foci per nucleus were indicated for each cell. The figures show the median values of cell populations ($n = 3$ with > 600 cells per sample) displaying a defined number of detected foci according the amount of Hoechst fluorescence. The significance of the differences in the number of foci between the control and treated cells or between the culture conditions was analyzed using a two-way ANOVA test with a Tukey correction.

Homologous Recombination

HR efficiency was calculated using a PCR-based HR assay kit (Norgen Biotek, Corp. provided by Interchim, Montlucon, France). The kit consists of two pUC19 plasmids (dl1 and dl2) harboring different mutations in their LacZ coding region. The plasmids were cotransfected into MSCs (2.5 μg of dl1 and 2.5 μg of dl2 per six-well plate) for 24 hours using Viromer Yellow transfection reagent (Lipocalyx provided by Interchim). Thereafter, total cellular DNA was isolated using a NucleoSpin TriPrep Kit (Macherey-Nagel, Hoerdt, France). The DNA concentration was evaluated using a NanoPhotometer (Implen provided by Evobiosystem, Les Ulis, France), and 150 ng of total DNA was used in PCR reactions containing either a set of universal primers amplifying all plasmid backbones or a set of specific primers targeting the sequence generated from the HR process of the mutated plasmids. PCR reactions were performed using a Q5 High-Fidelity DNA polymerase (New England Biolabs France, Evry, France) under the following conditions: initial denaturation at 98°C for 3 minutes; 35 cycles of 98°C for 15 seconds, 58°C for 30 seconds, and 72°C for 30 seconds; and a final extension at 72°C for 2 minutes. Amplified DNA (recombined sequence: 420 bp; backbone plasmid dl1: 546 bp and dl2: 258 bp) was loaded, stained with ethidium bromide, and submitted to densitometric analyses (GeneTools, Syngene provided by Ozyme). The HR efficiency was calculated by comparing the densitometric value of the recombinant product of each case versus that of sequences amplified using the universal primer set.

Osteogenic Induction

ADSCs and BM-MSCs were seeded at 1,000 cells/well in 96-well plates. Twenty-four hours later, ADSCs and BM-MSCs were cultured under normoxic conditions (37°C) and submitted to an osteogenic induction medium supplemented with penicillin (100 U/ml) and streptomycin (100 μg/ml; StemMacs OsteoDiff Media, human; Miltenyi Biotec) for 21 days. The media were changed every 3 days. At the end of the osteogenic induction period, the cells were washed twice with 1 × PBS and fixed in 4% paraformaldehyde solution at room temperature for 10 minutes. After the cells were washed three times, the mineralized matrix with calcium deposits was stained with an Alizarin Red solution (13.6 mg/ml, pH 4.1–4.3; Sigma-Aldrich). The cells were examined using an Olympus IX71 inverted microscope (Olympus, Tokyo, Japan) equipped with a × 10/0.25 Php lens. Images were acquired using an Olympus SC30 camera.

Statistical Analysis

Relative influences of oxygen levels and passages on ADSCs and BM-MSCs regarding DNA repair were evaluated using a two-way ANOVA test. Significance levels were determined using a Tukey or a Sidak post hoc test depending on the experiment. Unless otherwise indicated, the results represent the mean, with error bars showing the SD. The methods for obtaining PL, counting population doublings, determining clonogenic survival, cytogenetically analyzing MSCs, performing Western blot experiments and NHEJ assays, and analyzing mitochondrial DNA stability are described in Supporting Information.

Results

PL Improves the Generation of MSC Colonies Regardless of the Oxygen Tension

Before being used in clinical applications, MSCs need to fulfill several criteria including conserved genome integrity. Here, fully characterized clinical-grade ADSCs and BM-MSCs (CD90+, CD73+, and CD200−, CD271−) (Supporting Information Fig. S1A, S1B) were cultured in PL-containing media (Fig. 1A) and studied for their DDRs and DNA repair at the early (end P2) and middle (end P5) stages of their in vitro expansion depending on the oxygen tension (Fig. 1B).

At first, we evaluated the ability of ADSCs and BM-MSCs to generate colonies when cultured in fetal calf serum (FCS)-containing medium supplemented with basic fibroblast growth factor (bFGF) (Fig. 1C; Supporting Information Fig. S1C). At P2, the formation of colonies was significantly increased in ADSCs cultured in hypoxia (6.55% ± 1.71% in hypoxia vs. 3.34% ± 0.89% in normoxia) whereas BM-MSCs featured less colonies regardless of the oxygen tension (0.74% ± 0.49% in normoxia vs. 1.68% ± 0.87%). In comparison, PL-containing media improved the formation of colonies (Fig. 1D; Supporting Information Fig. S1D). However, the oxygen level did not significantly alter the colony formation in P2 ADSCs (13.16% ± 1.59% in normoxia vs. 10.08% ± 2.11% in hypoxia) and in P2 BM-MSCs (7.31% ± 0.54% under normoxic conditions vs. 7.19% ± 0.88% under hypoxic conditions). As could be expected, end P5 cells harboring 20 cumulative population doublings (CPDs) were less prone to generate colonies. Only 6.17% ± 0.63% of P5 ADSCs formed colonies in normoxia and 6.44% ± 2.46% in hypoxia. BM-MSCs at P5 formed approximately 1.5 times fewer colonies than those at P2 (Fig. 1D).

Thus, PL appeared to be more supportive for ADSC and BM-MSC cultures, regardless of the oxygen tension ($F = 1.382$), while hypoxia improved colony generation only when FCS and bFGF were used in ADSCs. However, even when cells cultured with PL kept proliferating until P7–P10 (Fig. 1B), the percentage of cells able to generate colonies decreased accordingly.

MSC Survival Following Genotoxic Stress Is Not Impaired by Hypoxic Culture Conditions

The survival of ADSCs and BM-MSCs cultured with PL was investigated following doxorubicin (Dox) treatment (Fig. 2A). The DSB-inducing agent Dox was used to cause genotoxic events that clinical-grade MSCs could undergo, to a lesser extent, during their expansion. The dose was chosen according

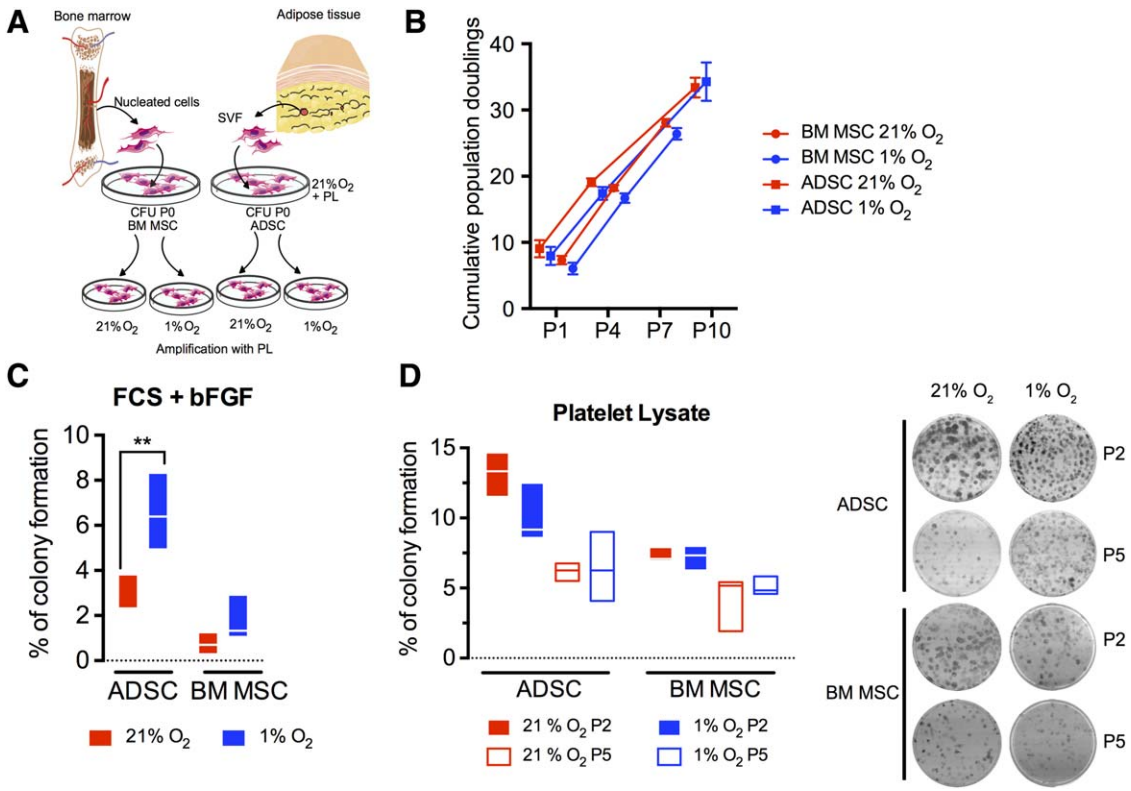

Figure 1. Colony formation ability of MSCs is increased by PL. **(A)**: A summary of protocols used for the isolation and culture of clinical-grade ADSCs and BM-MSCs. MSCs were expanded using PL under 21% or 1% O_2. **(B)**: Cumulative population doublings for ADSCs (squared dots, $n = 3$) and BM-MSCs (dots, $n = 3$) cultured with PL under 21% (red) or 1% (blue) O_2. The results represent the mean ± SD. **(C)**: Colony formation of P2 ADSCs ($n = 3$) and P2 BM-MSCs ($n = 3$) cultured with FCS and bFGF under 21% O_2 (red) or 1% O_2 (blue) with or without Dox treatment. Significance between normoxic and hypoxic culture conditions was assessed using a two-way ANOVA test followed by a Tukey post hoc test; **, $p < .01$. **(D)**: Colony formation efficiencies for ADSCs and BM-MSCs cultured with PL at the end of P2 and P5. Representative images from ADSC or BM-MSC colonies at the end of P2 and P5 are displayed. The graphs represent data from three donors for each cell type (21% O_2 in red and 1% O_2 in blue). Significance was assessed using a two-way ANOVA test followed by a Tukey post hoc test. Abbreviations: ADSC, adipose-derived stromal cell; bFGF, basic fibroblast growth factor; BM, bone marrow; CFU, colony-forming unit; MSC, mesenchymal stromal/stem cell; PL, platelet lysate; SVF, stromal vascular fraction.

to previous experiments demonstrating significant DNA damage and low survival in MSCs cultured with FCS-bFGF (Supporting Information Fig. S1C). Dox treatment greatly reduced ADSC colony formation at the end of P2 under normoxic (3.00% ± 0.79%) and hypoxic (2.25% ± 1.33%) conditions and P5 (1.14% ± 0.49% in normoxia vs. 1.02% ± 0.46% in hypoxia) (Fig. 2B, 2C). Similarly, the generation of BM-MSC colonies drastically decreased following Dox treatment (0.38% ± 0.07% under normoxic conditions and 0.24% ± 0.04% under hypoxic conditions). At the end of P5, colony formation decreased to 0.20% ± 0.08% under normoxic conditions and to 0.05% ± 0.03% under hypoxic conditions.

These data suggest that colony formation abilities of LP-cultured ADSC and BM-MSC were severely hindered by genotoxic stress such as DSBs. However, emergence of colonies from ADSCs and BM-MSCs suggest both MSCs overcame these events. Eventually, oxygen level had no effect on survival ($F = 1.382$) (Supporting Information Fig. S1D).

Hypoxia Differentially Modulates the DDR in ADSCs and BM-MSCs

Although limited, the emergence of colonies following genotoxic events suggested survival and likely substantial DNA repair abilities in the treated cells. Therefore, we investigated DNA damage signaling immediately after Dox treatment and 24 hours after the end of Dox treatment (Fig. 2A) in ADSCs (Fig. 3A, 3B; Supporting Information Fig. S2A, S2B) and BM-MSCs (Fig. 3C, 3D; Supporting Information Fig. S2C, S2D). The phosphorylated form of Chk2 (Thr68), which is directly targeted by the ATM/ATR complex, indicated efficient DDRs in ADSCs and BM-MSCs. Although not significant, densitometric analyses revealed that BM-MSCs at P2 and P5 cultured under hypoxic conditions showed greater Chk2 activation than ADSCs (Fig. 3A, 3C; Supporting Information Fig. S2A, S2C, S2E). Interestingly, the p-Chk2 signal lasted briefly under hypoxic conditions (Rec lanes). Consequently, p53 was phosphorylated on Ser15 after Dox treatment and weakened during the recovery time. Hypoxia hindered p53 activation in P2 BM-MSCs compared with ADSCs (Fig. 3A, 3C; Supporting Information Fig. S2E). However, the p-p53 difference between normoxia and hypoxia was no longer apparent at P5 (Supporting Information Fig. S2C, S2E). When cultured with FCS and bFGF, instead of PL, P2 ADSCs, and BM-MSCs featured similar remaining levels of p-p53 at 24 hours after Dox treatment, regardless of the oxygen tension (Supporting Information Fig. S2F). This result suggested that PL might modulate, to some extent, the DDR according to the oxygen level. Interestingly, HIF-1α silencing under hypoxic conditions increased the Dox-dependent p-Chk2 levels but slightly decreased p-p53 levels, indicating that p53 activation might not rely only on Chk2 activity (Supporting Information Fig.

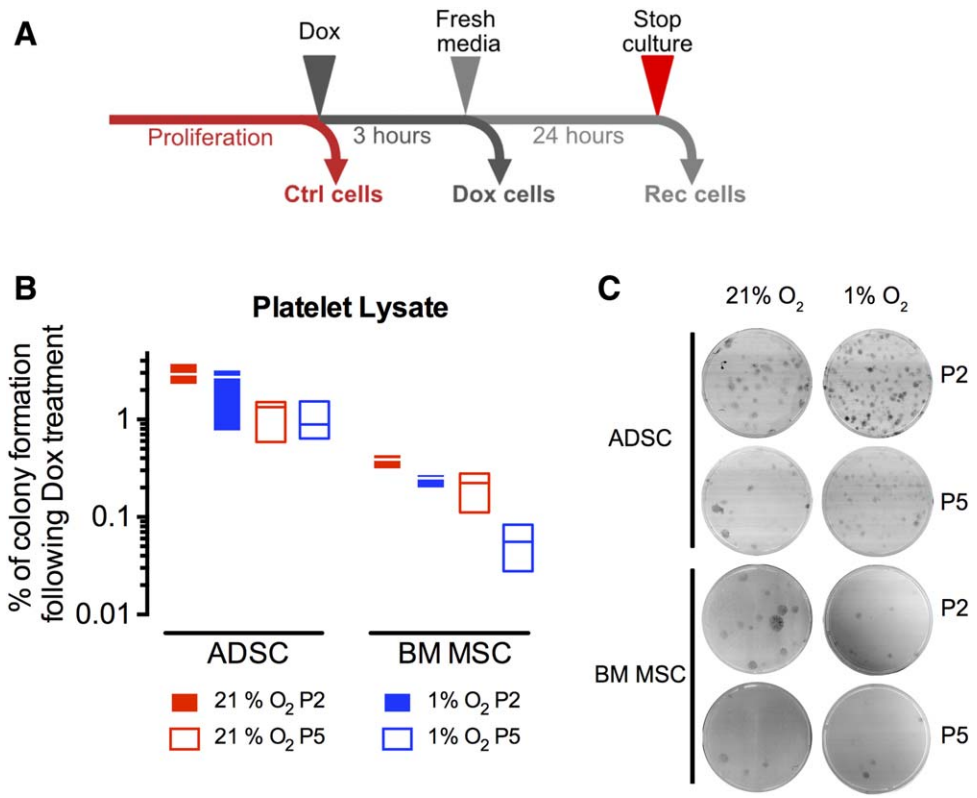

Figure 2. MSC survival is not affected by hypoxic culture conditions. **(A)**: Experimental protocol of survival assays following Dox treatment (Ctrl cells, control; Dox cells, Dox-treated cells for 3 hours; Rec cells, recovering cells 24 hours after stopping Dox treatment). **(B)**: Proliferating ADSCs and BM-MSCs cultured under 21% O_2 or 1% O_2 with platelet lysate were incubated at near confluence with Dox (Dox, 0.25 μM) for 3 hours. Then, the cells were plated at 60 and 500 cells per square centimeter. **(C)**: Representative images (60 cells per square centimeter) are displayed. The graphs represent data from three donors for each case (21% O_2 in red and 1% O_2 in blue). Significance was assessed on three donors for each type of cell using a two-way ANOVA test followed by a Tukey post hoc test (Supporting Information Fig. S1D). Abbreviations: ADSC, adipose-derived stromal cell; BM, bone marrow; MSC, mesenchymal stromal/stem cell.

S3A, S3B). Therefore, HIF-1α might oppose the DDR-dependent cell cycle blockade in clinical-grade MSCs by acting on p-Chk2 and p-p53 levels.

γH2AX Is Induced After Genotoxic Stress in MSCs, But ADSCs Display Greater ub-γH2AX Levels Under Hypoxic Conditions

In response to DNA damage, the local histone variant H2AX is phosphorylated on Ser139 to form DNA damage-associated γH2AX. Here, γH2AX protein levels increased in response to Dox, regardless of whether MSCs were cultured under 21% O_2 or 1% O_2. Twenty-four hours later, γH2AX levels decreased in both ADSCs and BM-MSCs at both P2 and P5 but without recovering to control levels (Fig. 3A–3D; Supporting Information Fig. S2A–S2D). The same pattern was observed in ADSCs and BM-MSCs when cultured with FCS and bFGF instead of PL (Supporting Information Fig. S2F). However, the γH2AX ubiquitylated form (ub-γH2AX), which has been shown to leave damaged DNA [22], was greatly augmented under hypoxic conditions in response to Dox treatment or during recovery following Dox treatment, particularly in ADSCs (P2 and P5; Fig. 3A, 3B; Supporting Information Fig. S2A, S2B), leading to an increased ratio of ub-γH2AX on γH2AX compared with BM-MSCs (Fig. 3C, 3D; Supporting Information Fig. S2C, S2D). Therefore, the oxygen tension appeared to be responsible for the distinct ubiquitylation status of γH2AX after genotoxic stress noticed between ADSCs and BM-MSCs at least at P2 (respectively $F = 6.441$ vs. $F = 0.5818$). Moreover, the discrepancies observed between ADSCs and BM-MSCs under hypoxic conditions might be due to different hypoxic responses involving HIF-1α. Indeed, ub-γH2AX remained present in the absence of HIF-1α in ADSCs, unlike in BM-MSCs (Supporting Information Fig. S3A, S3B).

Different Patterns of DNA Damage-Induced γH2AX Foci Are Observed in BM-MSCs and ADSCs Cultured Under Hypoxic Conditions

Automatic analyses of γH2AX foci allowed for the localization of the DNA-damaged sites in ADSCs at P2 and P5 (Fig. 4A; Supporting Information Fig. S4A). Nuclei harboring more than four γH2AX foci were considered significantly damaged (Fig. 4B; Supporting Information Fig. S4B). As expected, γH2AX foci in control ADSCs were barely detectable under normoxic or hypoxic conditions. Following Dox treatment, numerous small foci scattered all over P2 or P5 ADSCs cultured under normoxia (Fig. 4A; Supporting Information Fig. S4B). Normoxic conditions significantly increased by approximately 1.5 times the frequency of damaged ADSC nuclei compared with those under hypoxic conditions ($F = 35.01$) (Fig. 4B; Supporting Information Fig. S4B). Then, we grouped ADSC nuclei according to oxygen tension in bins of 0–4, 5–10, 11–15, 16–20, and >20 γH2AX foci to better characterize the DDR (Fig. 4C; Supporting Information Fig. S4C). Following Dox treatment, ADSC nuclei primarily harbored more than 15 foci under normoxic

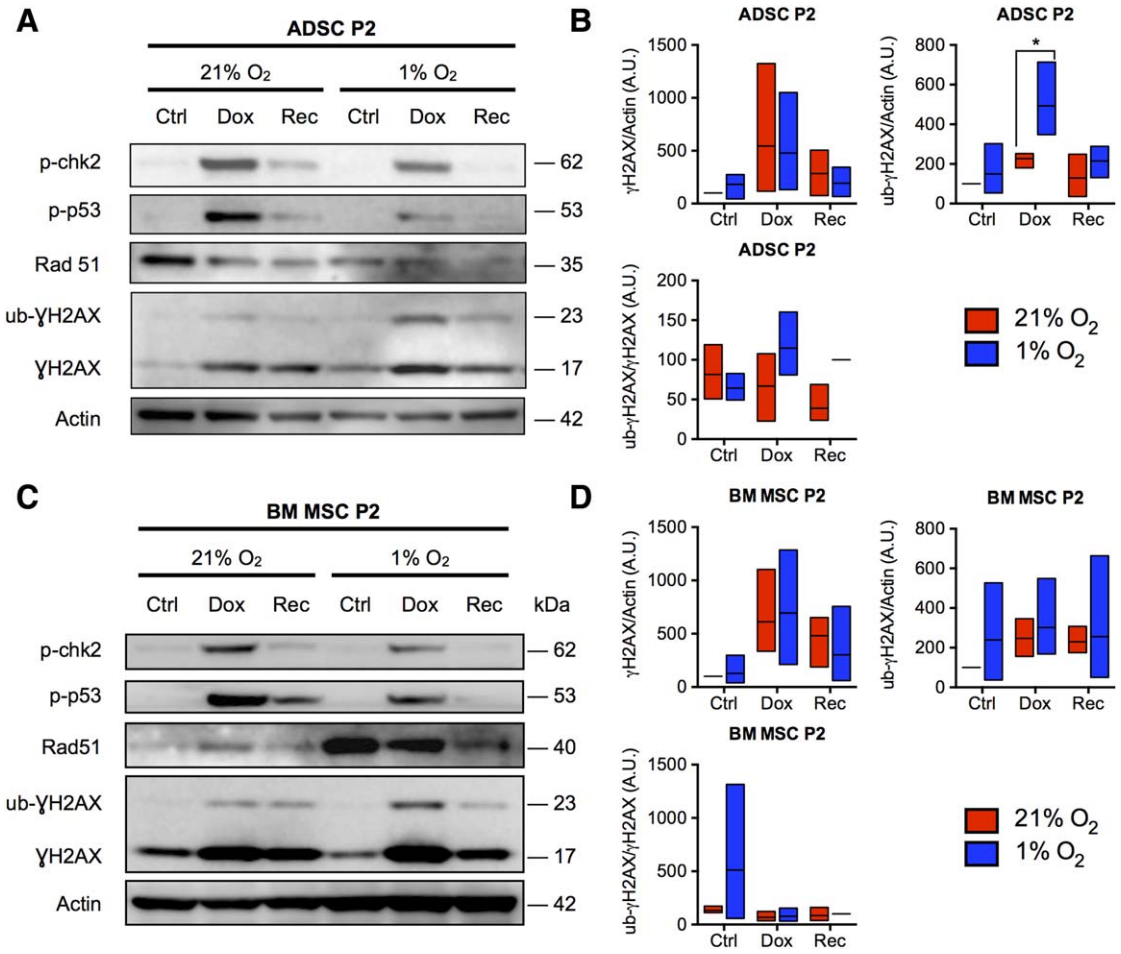

Figure 3. DNA damage response is altered in MSCs submitted to genotoxic stress under hypoxic conditions. **(A)**: Western blot analysis of DNA damage signaling factors in P2 ADSCs. Whole cell lysates from P2 cells cultured under 21% O_2 or 1% O_2 and exposed to Dox or unexposed were subjected to Western blot analysis for p-Chk2, p-p53, Rad51, γH2AX, and Actin (for loading controls). **(B)**: Densitometric analysis of γH2AX and ub-γH2AX from three Western blot experiments. Significance was assessed using a two-way ANOVA test followed by a Sidak post hoc test; *, $p < .05$. **(C, D)**: The same experiments as in (A) and (B) were performed with P2 BM-MSCs. Abbreviations: ADSC, adipose-derived stromal cell; BM, bone marrow; MSC, mesenchymal stromal/stem cell.

conditions, while they primarily harbored less than 10 foci under hypoxic conditions. Twenty-four hours after the treatment was stopped, the foci increased in size. However, ADSCs featuring more than four foci kept increasing under hypoxic conditions and primarily harbored 5–10 foci, while normoxic conditions appeared to support the resolution of γH2AX foci, as suggested by the increasing rates of ADSCs harboring 0–4 foci and 5–10 foci (Fig. 4A–4C; Supporting Information Fig. S4A–S4C).

Almost all control BM-MSCs featured less than four γH2AX foci (Fig. 4D, 4E; Supporting Information Fig. S4D, S4E). Similar to ADSCs, the rates of BM-MSC nuclei with more than four γH2AX foci drastically increased following Dox treatment under normoxia, as suggested by the doubled amount of damaged nuclei than under hypoxic conditions (Fig. 4D, 4E; Supporting Information Fig. S4D, S4E). Here again, changes in the oxygen tension appeared to significantly modulate the γH2AX focal accumulation and resolution ($F = 213.43$). However, the nuclei rarely featured more than 15 γH2AX foci under normoxic conditions and 10 foci under hypoxic conditions (Fig. 4F; Supporting Information Fig. S4F). Eventually, after 24 hours of recovery, almost all BM-MSCs contained less than four foci under hypoxic conditions, while the remaining nuclei under normoxic conditions still featured 5–10 foci.

The frequencies of nuclei with more than four γH2AX foci under normoxic or hypoxic conditions, following doxorubicin treatment, were not significantly different at P5 (two-way ANOVA analyzes, F values < 2.74) excepting BM-MSCs in normoxia ($F = 3.36$). The dynamics of γH2AX foci contrasted between ADSCs and BM-MSCs under hypoxic conditions, suggesting BM-MSCs better signaled and repaired DNA damage while ADSCs kept accumulating γH2AX foci until 24 hours after the end of genotoxic stress.

53BP1 Foci Formation Following Genotoxic Stress and Their Resolution Are Not Modulated by Oxygen Tension

53BP1 is an early DDR protein whose recruitment occurs generally because of previous γH2AX foci formation. 53BP1 operates at the junction of NHEJ and HR repair processes, depending on the cellular input and context [23]. In all cases, approximately 90% of ADSCs at P2 and P5 contained more than four 53BP1 foci per nucleus, regardless of the oxygen

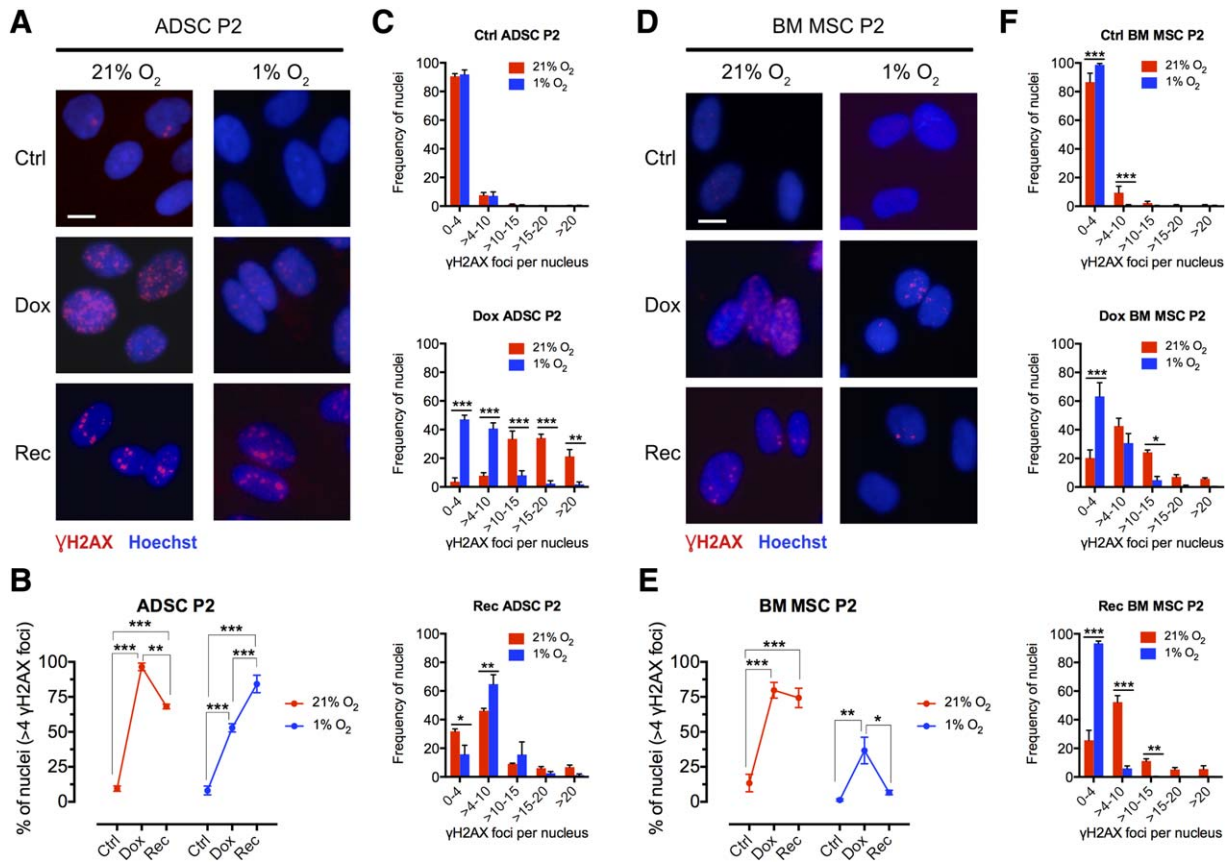

Figure 4. Hypoxia differentially modulates γH2AX foci accumulation and resolution in ADSCs and in BM-MSCs cultured with platelet lysate (PL). **(A)**: Representative images of γH2AX foci in nuclei from P2 ADSCs cultured under 21% O_2 or 1% O_2 in PL. Ctrl, Dox, and Rec nuclei were subjected to γH2AX immunofluorescence. Scale bar = 20 μm. **(B)**: Frequencies of significantly damaged nuclei (more than four γH2AX foci) in P2 cells cultured under 21% O_2 (red) or 1% O_2 (blue). The number of foci per nucleus was counted for at least 600 each of Ctrl, Dox, and Rec nuclei using ArrayScan ($n = 3$ donors, mean ± SD). Effects of the treatments were assessed. **(C)**: Distribution of Ctrl, Dox, and Rec nuclei with respect to their γH2AX foci numbers depending on the oxygen tension ($n = 3$, mean ± SD). **(D–F)**: The same experiments were performed with P2 BM-MSCs. Significance was assessed using a two-way ANOVA test followed by a Tukey post hoc test; *, $p < .05$; **, $p < .01$; ***, $p < .001$. Abbreviations: ADSC, adipose-derived stromal cell; BM, bone marrow; MSC, mesenchymal stromal/stem cell.

tension (Fig. 5A, 5B; Supporting Information Fig. S5A, S5B). Control ADSCs primarily displayed 5–15 foci per nucleus whereas in response to Dox treatment, the rates of significantly damaged nuclei increased for all conditions, with more than 15 foci per nucleus. These 53BP1 accumulations at DNA damage sites were independent of the total 53BP1 protein levels that were conserved with passaging, regardless of the conditions (Supporting Information Fig. S3C–S3F). Eventually, after the 24-hour recovery period, the percentages of significantly damaged nuclei were identical to the control (Ctrl), regardless of the oxygen tension. Thus, ADSCs presented primarily 5–10 foci per nucleus (Fig. 5C; Supporting Information Fig. S5C).

Comparatively, control nuclei with more than four 53BP1 foci represented less than 70% of BM-MSCs under 21% O_2 or 1% O_2 (Fig. 5D, 5E; Supporting Information Fig. S5D, S5E). However, BM-MSCs had fewer foci compared with ADSCs (0–10; Fig. 5F; Supporting Information Fig. S5F). Similar to ADSCs, Dox-dependent 53BP1 accumulation at DNA damage sites without affecting the total protein amount was observed in BM-MSCs cultured under normoxic or hypoxic conditions at P2 and P5 (Supporting Information Fig. S3D, S3F). Finally, the frequency of BM-MSC nuclei with more than four 53BP1 foci slightly decreased (Fig. 5D, 5E; Supporting Information Fig. S5D, S5E). However, similar to ADSCs, the frequency of Rec BM-MSC nuclei featuring 5–10 foci equaled that of Ctrl BM-MSCs (Fig. 5E, 5F; Supporting Information Fig. S5E, S5F). In addition, only approximately 20% of BM-MSC nuclei exhibited 0–4 foci, suggesting that the 24 hours recovery period was insufficient to perform a complete resolution of 53BP1 foci.

In conclusion, the oxygen tension had no significant effect on 53BP1 foci formation and resolution for ADSCs and BM-MSCs (excluding P5 ADSCs all F values < 3.17). Moreover, similar to γH2AX, the 53BP1 foci dynamics were not impaired, at least until P5 (all F values < 3.64).

γH2AX and 53BP1 Foci Accumulation Following Genotoxic Stress Further Increases During DNA Replication

Damaged nuclei were sorted according to their DNA content using Hoechst fluorescence intensity. ADSCs and BM-MSCs were mainly found in G1 at end P2 and P5 (Fig. 6A, 6B; Supporting Information Fig. S6A, S6B) but G2 cells significantly accumulated more γH2AX or 53BP1 foci (Fig. 6C, 6D; Supporting Information Fig. S6C, S6D; adjusted p values are presented in Supporting Information Tables S2, S3 and Fig. S8). In

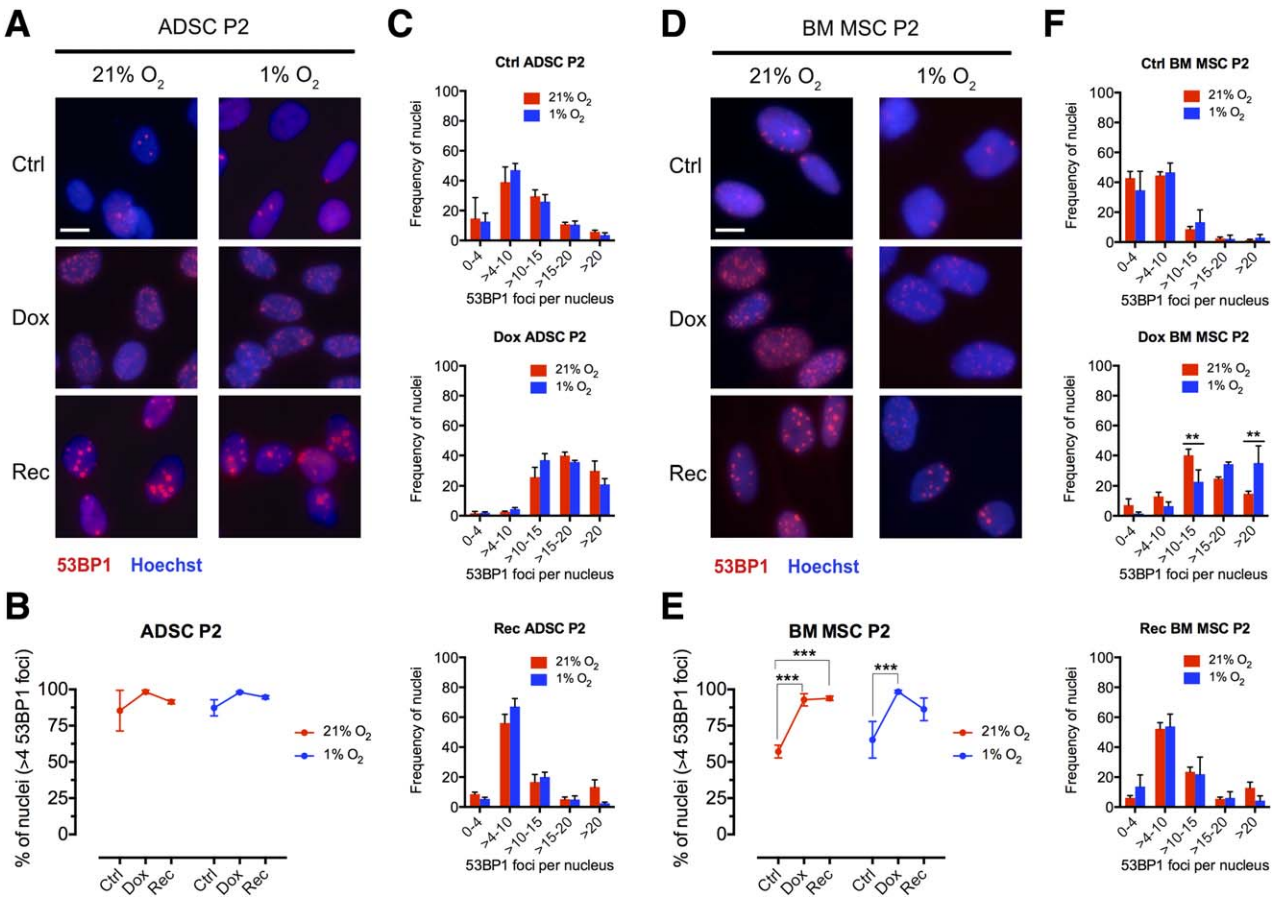

Figure 5. Hypoxia does not affect 53BP1 accumulation and resolution at DNA damage sites in MSCs when cultured under hypoxic conditions. **(A)**: Representative images of 53BP1 foci in nuclei from P2 ADSCs cultured under 21% O_2 or 1% O_2 in platelet lysate. Ctrl, Dox, and Rec nuclei were subjected to 53BP1 immunofluorescence. Scale bar = 20 μm. **(B)**: Frequencies of significantly damaged nuclei (more than four 53BP1 foci) in P2 cells cultured under 21% O_2 (red) or 1% O_2 (blue). The number of foci per nucleus was counted for at least 600 each of Ctrl, Dox, and Rec nuclei using ArrayScan analysis ($n = 3$ donors, mean $\pm$ SD). Effects of the treatments were assessed. **(C)**: Distribution of Ctrl, Dox, and Rec nuclei with respect to their 53BP1 foci numbers depending on the oxygen tension ($n = 3$, mean $\pm$ SD). **(D–F)**: The same experiments were performed with P2 BM-MSCs. Significance was assessed using a two-way ANOVA test followed by a Tukey post hoc test; **, $p < .01$; ***, $p < .001$. Abbreviations: ADSC, adipose-derived stromal cell; BM, bone marrow; MSC, mesenchymal stromal/stem cell.

control, G1 cells mainly presented 0–4 γH2AX foci. Conversely, moderate DNA damages, marked by >4–10 γH2AX foci, increased in G2 except for BM-MSCs cultured in hypoxia (Fig. 6C; Supporting Information Figs. S6C, S8 and Table S2). Then, γH2AX foci accumulated in response to doxorubicin. However, cells with > 20 γH2AX foci were rather observed in G2 in normoxia while in G1, ADSCs mainly featured 10–15 γH2AX foci and BM-MSCs 4–10 γH2AX foci. As a result of the hypoxic condition, the proportion of ADSCs and BM-MSCs featuring numerous foci was reduced following Dox. However, G2 cells contained more γH2AX foci while higher rates of cells with 0–4 foci were in G1. Eventually, rates of MSCs with numerous foci decreased at the end of the recovering time (Rec). Frequencies of cells with >4–10 foci were enhanced in G1, especially for ADSCs. Conversely, cells containing more than 15 γH2AX foci increased in ADSCs and BM-MSCs in G2.

The accumulation of 53BP1 foci according to cell cycle was evaluated as well (Fig. 6D; Supporting Information Fig. S6D, S8; Table S3). Control BM-MSCs in G2 were less prone to feature 0–4 53BP1 foci. Again, frequencies of ADSCs featuring from 4 to 10 53BP1 foci improved in G1. In comparison, 53BP1 foci rather increased in G2 cells, as suggested by elevated rates of >20 53BP1 nuclei. Doxorubicin treatment promoted 53BP1 foci. Interestingly, the > 10–15 and 15–20 53BP1 foci groups were more represented in G1, especially for ADSCs, whereas almost G2 cells contained more than 20 foci (Supporting Information Table S3). Eventually, Rec cells harboring between 4 and 10 53BP1 foci were particularly observed in G1 whereas remaining cells with more than 20 foci were in G2.

In conclusion, ADSCs and BM-MSCs accumulated more foci as the DNA content increased, regardless of the oxygen tension ($F = 298.6$ for γH2AX and $F = 854$ for 53BP1). These DNA damages occurring during replication are common for ADSC and BM-MSC and are still present at P5.

Low Oxygen Tension Is Required for the DNA Repair Activity of BM-MSCs

BM-MSCs and ADSCs were shown to behave differently under hypoxic conditions according to their accumulation and resolution of γH2AX foci in response to genotoxic stress. As previously reported [5], karyotype analyses demonstrated that chromosomal abnormalities in MSCs were more dependent on the donor origin than on culture conditions. Interestingly, normal karyotypes were detected more frequently in BM-MSCs than in

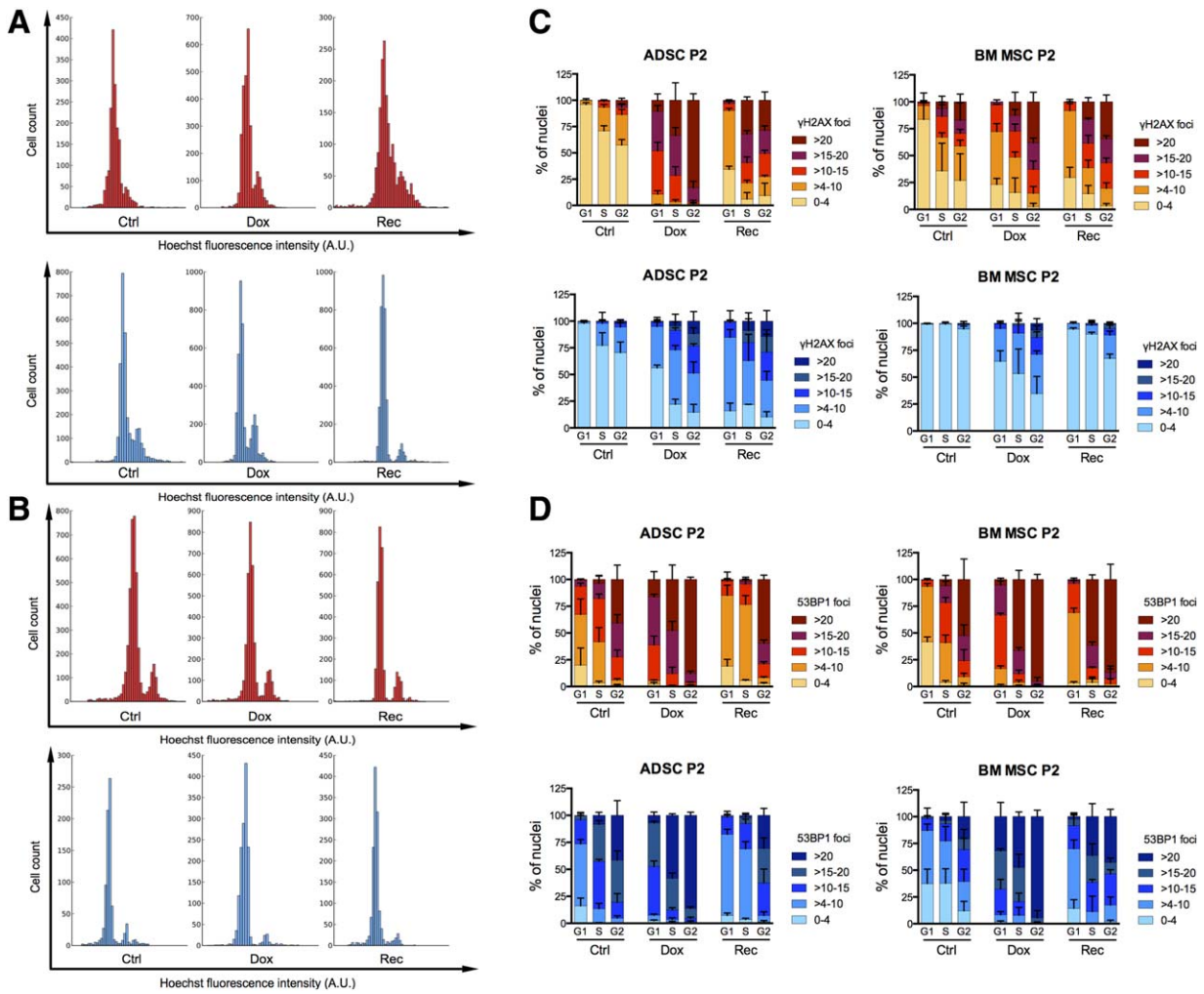

Figure 6. γH2AX and 53BP1 foci accumulation in nuclei following genotoxic stress further increases during DNA replication. **(A, B)**: Representative cell cycle distributions obtained after Hoechst staining and ArrayScan quantification of P2 ADSCs (A) or P2 BM-MSCs (B) cultured with platelet lysate under 21% O_2 or 1% O_2. **(C)**: ADSCs and BM-MSCs from Ctrl, Dox, and Rec cases were sorted with respect to G1, S, and G2/M phases and to γH2AX foci number per nucleus (0–4; > 4–10; > 10–15; > 15–20; and >20). **(D)**: P2 ADSCs and BM-MSCs were analyzed for 53BP1 as in (C). Normoxic and hypoxic conditions are represented by shades of red and blue, respectively. The stacked bars represent the mean ± SD from three different donors (Supporting Information Tables S2, S3). The differences between G1 and G2 cells were analyzed in three donors for each type of cell using a two-way ANOVA test and a Tukey post hoc test (Supporting Information Tables S2, S3, Fig. S8). *F* values confirming more occurrences of >20 foci cells in G2, in comparison with G1, were obtained using a two-way ANOVA test corrected with the Sidak method. Abbreviations: ADSC, adipose-derived stromal cell; BM, bone marrow; MSC, mesenchymal stromal/stem cell.

ADSCs (Supporting Information Table S1). Therefore, we hypothesized that DNA repair activities could be differentially modulated between the two cell types. First, hypoxic conditions, in comparison with normoxic conditions, upregulated the expressions of the NHEJ participants *XRCC5* (Ku80) ($F = 74.35$), *DCLRE1C* (Artemis) ($F = 22.83$), and *TP53BP1* (53BP1) ($F = 175.3$) in BM-MSCs, while these mRNA levels globally decreased in ADSCs in the same context ($F = 41.61$ for *XRCC5*, and 10.47 for *DCLRE1C*) (Supporting Information Fig. S7A). Eventually, the expression of the late NHEJ marker *LIG4* (DNA Ligase IV) was not modulated by oxygen tension in ADSCs ($F = 1.55$) and in BM-MSCs ($F = 1.02$). Again, these expression levels were moderately impacted by passages. Eventually, the benefits of hypoxia on the expression of NHEJ markers in BM-MSCs were confirmed by a significant upregulation of the NHEJ activity ($F = 18.01$) (Fig. 7A).

Homologous recombination (HR) ensures error-free DNA repair. BM-MSCs were again distinguished from ADSCs under hypoxic conditions by the upregulated expression levels (all *F* values > 18) of *BRCA1, RBBP8* (CtIP), and *RAD51*, whose increase was also confirmed at the protein level (Fig. 3A, 3C; Supporting Information Figs. S2A, S2C, S2E, S7A). Accordingly, the HR efficiency increased for all the tested BM-MSCs when cultured under hypoxic conditions and remained the same at P5. By contrast, hypoxia poorly influenced the HR efficiency in ADSCs P2 but decreased it at P5 (Fig. 7B).

Low Oxygen Tension Favors the Stability of BM-MSC mtDNA and Maintains the Differentiation Potential of ADSCs and BM-MSCs

Mitochondrial functions and biogenesis correlate with the regulation of metabolism, apoptosis, and stem cell renewal. Here,

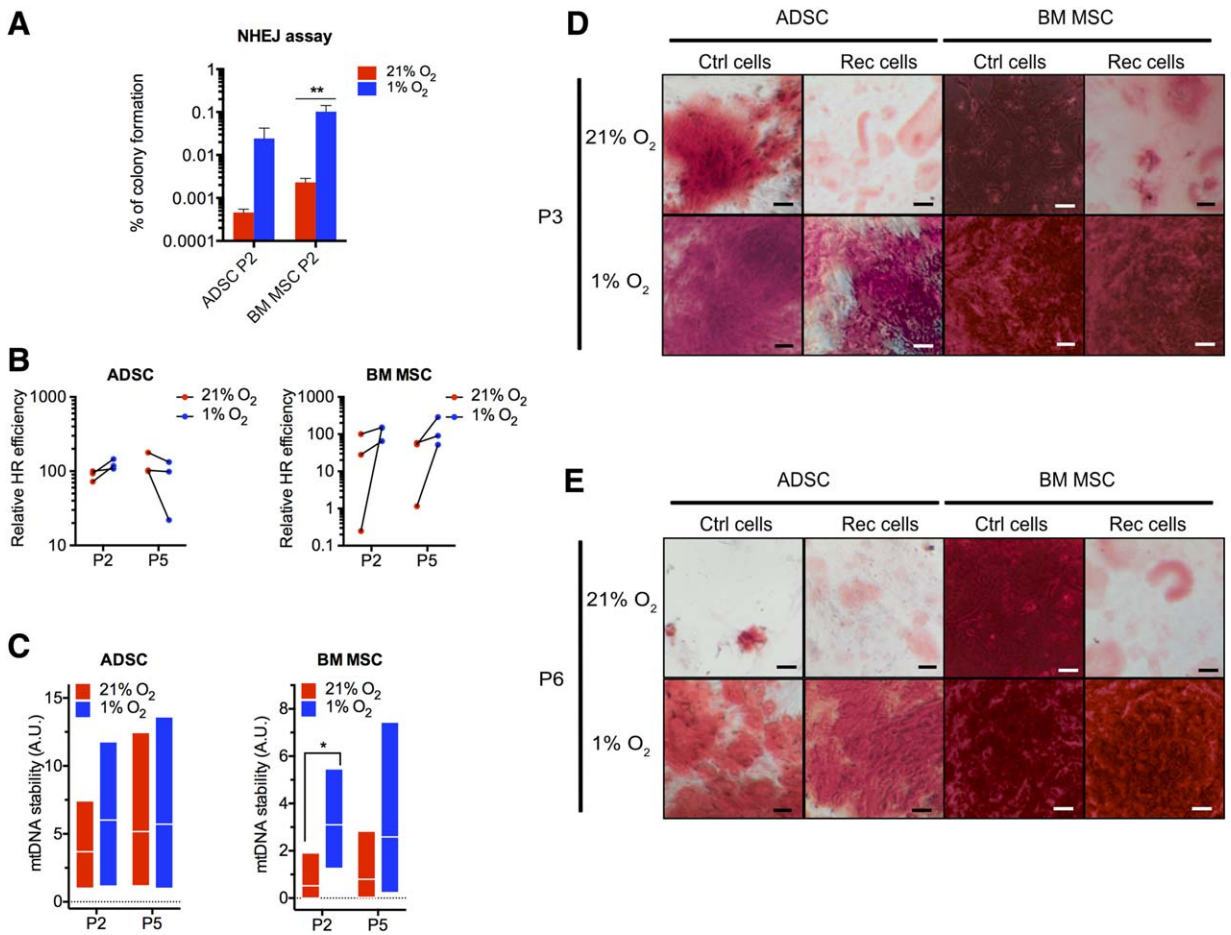

Figure 7. Hypoxia improves DNA repair and mitochondrial DNA stability of BM-MSCs, but improves differentiation potentials of ADSCs and BM-MSCs following genotoxic stress. **(A)**: Nonhomologous end joining efficiency in P2 ADSCs and BM-MSCs as determined by the formation of colonies following the integration of a linearized pEGFP-C1 plasmid and selection with G418. The results indicate the relative colony formation efficiency for every donor at P2 under 21% O_2 (red) and 1% O_2 (blue). Effect of oxygen tension was analyzed using a two-way ANOVA test followed by a Sidak post hoc test: ***, $p < .01$. **(B)**: HR efficiency in ADSCs and in BM-MSCs as determined by an in vivo plasmid-based recombination reporter assay. The results indicate the relative HR efficiency for every donor at P2 and P5 under 21% O_2 (red) and 1% O_2 (blue). **(C)**: Mitochondrial DNA stability in ADSCs and BM-MSCs. mtDNA integrity was measured by the relative amplification efficiency of a 6.141-kb mtDNA fragment compared to a 454 bp mtDNA fragment. PCRs were performed twice on two initial batches of ADSCs ($n = 3$) and BM-MSCs ($n = 3$) cultured independently under 21% O_2 (red) and 1% O_2 (blue). Means of mtDNA stabilities between normoxic and hypoxic conditions were analyzed using a two-way ANOVA test followed by a Sidak post hoc test; *, $p < .05$. **(D, E)**: Osteoblast differentiation of ADSCs and BM-MSCs after genotoxic stress. ADSCs and BM-MSCs were submitted to Dox treatment under the same culture conditions as described in Figures (1 and 2). Ctrl and Rec cells underwent osteogenic induction for 21 days under normoxic conditions (P3 and P6). Osteoblast-specific calcium deposits were stained with Alizarin Red. Scale bar = 50 μm. Experiments were performed for the three donors of each group; a representative image is shown. Abbreviations: ADSC, adipose-derived stromal cell; BM, bone marrow; HR, homologous recombination; MSC, mesenchymal stromal/stem cell.

BM-MSCs cultured in hypoxia specifically improved the stability of their mitochondrial DNA (mtDNA) ($F = 9.03$) especially at P2 ($p = .0414$). This hint that the mtDNA sequence encompassing from the D-Loop to *COX1 locus* might have accumulated less base alterations during the BM-MSCs expansion, helping its amplification during PCR experiments (Fig. 7C; Supporting Information Fig. S7B). In comparison, various oxygen tensions did not influence the mtDNA stability in ADSCs ($F = 0.54$) (Fig. 7C). Eventually, changes in the relative mtDNA stabilities between passage 5 and passage 2 were not found meaningful either for BM-MSCs ($F = 0.03$) or for ADSCs ($F = 0.09$).

Under ex vivo expansion, MSCs can experience a loss of genomic stability, senescence, immunomodulatory properties, and differentiation potential. Therefore, we evaluated whether culture conditions associated with the induction of DNA damage could impair the MSC differentiation potential. After Dox treatment, the control and treated cells were plated and recovered for 10 days under normoxic or hypoxic conditions (Ctrl and Rec cells, respectively; as in Fig. 2) before osteogenic induction at P3 and P6. Control BM-MSCs at P2 and, to a lesser extent, ADSCs cultured under normoxic conditions differentiated into osteoblasts as evidenced by the mineralized matrix stained with Alizarin Red. Conversely, Rec cells under normoxic conditions scarcely differentiated (Fig. 7D). The osteogenic differentiation for cells at P6 under normoxic conditions led to similar results (Fig. 7E). Strikingly, Ctrl and Rec cells from colonies generated under hypoxic conditions efficiently differentiated until P6. In contrast, we performed adipogenic induction (Supporting Information Fig. S7C), and, interestingly, the efficiency of the adipogenic induction of ADSCs and BM-MSCs increased when they

were previously expanded under hypoxic conditions. Taken together, these results suggest that hypoxia favors recovery from genotoxic stress and allows for the conservation of the differentiation potential of MSCs.

Discussion

Although MSCs are found in several tissues, they are scarce and require ex vivo expansion to conform to clinical needs. These steps may increase phenotypic loss, replicative stress, or DNA damage [24]. Maintenance of MSC properties is critical and specific culture conditions have been established to prevent low survival engraftment and replicative stress issues [15, 25, 26]. The use of hypoxia remains controversial; several studies have reported that hypoxia either compromised genomic stability [20] or had no significant effect [27]. In addition, spontaneous transformations of human MSCs during in vitro expansions have been reported, but these results were not confirmed by other studies [5, 8] and were finally retracted [28].

Few studies have addressed the DDRs and DNA repair in human MSCs [29]. Here, we analyzed the DDR and DNA repair processes in clinical-grade ADSCs and BM-MSCs during their long-term expansions under 21% O_2 or 1% O_2. Human PL is enriched with growth factors (TGFβ, bFGF, and PDGFs) and was used instead of FCS-bFGF to minimize prion or virus transmission and contact with xenogenic proteins [30]. In accordance with previous studies, ADSCs were cultured with 2% PL and BM-MSCs with a higher concentration [3, 31, 32]. ADSCs and BM-MSCs cultured with PL showed similar CPDs for all studied passages regardless of the oxygen tension, and generated more CFU-F than with FCS-bFGF.

Following genotoxic stress both ADSCs and BM-MSCs survival rates decreased the same way under 21% or 1% O_2, as suggested by conserved p53 activation until end P5 [33]. However, HIF-1α in hypoxia might prevent cell cycle arrest by decreasing p-Chk2 levels and might modulate ATM activities [34]. 53BP1 and γH2AX foci appeared in response to genotoxic stress, indicating an effective DDR and further accumulated when ADSCs and BM-MSCs were replicating. However, BM-MSCs cultured in hypoxia demonstrated moderate γH2AX foci accumulation and efficient resolution of foci. Conversely, rates of damaged ADSCs ($>$4 foci) kept increasing at 24 hours post-Dox treatment, which was consistent with delayed DDR reported in irradiated fibroblasts continually exposed to hypoxic conditions [33].

ADSCs presented elevated ub-γH2AX levels under hypoxic conditions that were not consistent with γH2AX and 53BP1 foci kinetics observed either in ADSCs under normoxic conditions or in BM-MSCs. Usually, the ubiquitylation results from the activity of ubiquitin ligases (RNF8, RNF168) recruited by MDC1 at DSBs and renders the chromatin permissive for the downstream elements of DNA repair [35, 36]. Studies emphasized that efficient resolution of γH2AX foci depends on direct or indirect deubiquitinating (DUB) activities. Thus, defective or delayed resolution of γH2AX foci was observed in absence of USP45 or ERCC1 [37]. Exploring USP45 activities on ub-γH2AX in hypoxia could provide new insights regarding γH2AX regulation [38]. However, ub-γH2AX levels in ADSCs in hypoxia were not dependent on HIF-1α, which indicates that potential ubiquitin ligases or DUB proteins might rely on other HIFs. In addition, evaluating the UBR5 and TRIP12 status in ADSCs in hypoxia during recovery might help to determine whether remaining ub-γH2AX labels intact DNA. Indeed, UBR5 and TRIP12 prevent excessive spread and accumulation of ubiquitin-regulated genome caretakers toward undamaged DNA sites [39]. Unlike γH2AX, 53BP1 foci were already observed in control BM-MSCs and ADSCs. However, the 53BP1 foci dynamics appeared unaffected by changes in the oxygen tension. Therefore, post-translational modifications involving ATM or DNA-PKc activity [40–42], SUMOylation events [43], or specific chromatin contexts [13, 44] remain to be explored to determine specifics discrepancies between 53BP1 and γH2AX recruitments in MSCs.

Cell origin, culture media, microenvironment, and acute or chronic exposure to hypoxia represent several criteria that have prevented the emergence of a consensus regarding the impact of oxygen tension on DNA integrity. Hypoxia was reported to downregulate HR-related gene expression (*BRCA1, RAD51*) in cancer cells, resulting in DNA repair impairments [18, 19, 45, 46]. Moreover, studies involving human BM-MSCs and ADSCs have proposed that passage and primarily hypoxia exposure time might hinder mismatch repair (MMR) via *MHL1* or *MSH6* downregulation, HR by decreasing *BRCA1* and *RAD51* expression or NHEJ by reducing *DNA-PKc, LIG4*, and *XRCC5* (*Ku80*) mRNA levels [20, 29, 47]. In PL-cultured clinical-grade BM-MSCs, expression of HR markers (*BRCA1, RBBP8*, and *RAD51*) and HR activity were upregulated under hypoxic conditions. Interestingly, improved cell survival and DNA repair following ionizing radiation were previously reported in murine BM-MSCs cultured under mild hypoxic conditions (2%–5% O_2) together with HIF-1α-mediated Rad51 accumulation [17]. In contrast, clinical-grade ADSCs displayed lower *BRCA1, RBBP8*, and *RAD51* mRNA expression and HR activity. Likewise, BM-MSCs under hypoxic conditions presented increased *DCLRE1C* and *XRCC5* mRNAs levels but also displayed improved NHEJ activity, whereas these genes were downregulated or stable in ADSCs. Nevertheless, karyotype analyses demonstrated more frequent chromosomal alterations in ADSCs than in BM-MSCs under all conditions. These results suggest a predominance of the donors over the culture conditions and more reliable DNA signaling or repair capacities in BM-MSCs. Mitochondrial DNA stability was also evaluated during MSC expansion. Low O_2 concentrations promote the shift from oxidative phosphorylation toward anaerobic glycolysis [48] and lower ROS release, that would benefit the mtDNA stability. No sizeable deletion was detected in mtDNA from ADSCs and BM-MSCs either under normoxia or hypoxia (not shown). Correct PCR amplifications suggest that mtDNA copies are unaffected by prior base damage, modifications, or mutations, which are typically responsible for replication errors or hindrance [49]. Here, mtDNA copies from BM-MSCs cultured in hypoxia seemed to less accumulate damage that might hinder their amplifications, resulting in greater mtDNA stability. Thus, reproducing at least partially the stem cell niche might be of interest for the efficient repair of mtDNA lesions [50]. Accordingly, hypoxia would limit the emergence and the propagation of mtDNA defects toward daughter or surrounding cells [51] and particularly delay aging of BM-MSCs [52]. Taken together, even when MMR was not considered, only BM-MSCs displayed increased levels of genomic and mtDNA stabilities when cultured under hypoxia.

Unexpectedly, only hypoxic culture conditions promoted the expansion of multipotent MSCs following DNA damage induction. However, we did not confirm if hypoxia increased

DNA repair activities of these cells, as suggested by the several results observed in BM-MSCs but not in ADSCs, or rather exerted a selection among a heterogeneous cell population of few cells that intrinsically possessed elevated DNA repair and proliferative capacities. This latter example could then explain some ADSC features.

Conclusion

Collectively, our results revealed that culture protocols need to be suitably selected for in vitro expansions of MSCs, depending on their tissue origins. Contrasting hypoxic responses suggested that cognate BM-MSC and ADSC niches might provide specific paracrine factors and O_2 concentrations. BM-MSCs reacted positively to low O_2 tensions, with increased DNA repair protein expression and efficient DNA repair and mtDNA maintenance. Conversely, the hypoxic response of ADSCs was less clear. Here, we showed that hypoxia promoted survival and differentiation following DNA lesions, while the PL effects were more pronounced during the self-renewal process. In brief, direct expansion of isolated ADSCs in hypoxia appeared less relevant with regard to DNA repair capacities compared with BM-MSCs. Additional studies should determine the oxygen levels suitable for benefiting the MSC phenotype and stabilizing DNA repair events according to the MSC source.

Acknowledgments

This work was supported by the ANR program (SAFE 2012) (ANR-11-RPIB-0012) whose recipients are N.B., M.P., S.L., M.L.R., L.S., K.T., and R.P. The authors N.B., S.L., R.P., and K.T. are also supported by grants from the Université Rennes 1 (Emerging Scientific Challenges 2013) and L.B. and M-L. R. by "Contrat de recherche laboratoire-entreprise Région Midi-Pyrénées n° 12050983 NOMASEC". A.M. is the recipient of a doctoral fellowship from La Région Bretagne and La Ligue Contre le Cancer (Bretagne). K.T. and L.S. are also supported by ECELLFRANCE (ANR-11-INSB-005) and by the European Center for Transplantation Sciences and Immunotherapy (IHU CESTI, ANR-10-IBHU_0005). R.P. is supported by AIS Rennes Métropole, INSERM (Institut National de la Santé et de la Recherche Médicale), La Ligue Contre le Cancer (Grand Ouest), and the Association pour la Recherche sur le Cancer.

Author Contributions

N.B.: study conception and design, data collection, assembly, analysis, and interpretation, and manuscript writing and editing; A.M., M.P., S.L., M.L.R., and R.L.: study material provision and data collection; L.S. and K.T.: study conception and design and data collection and assembly, financial support, manuscript editing, and final manuscript approval; R.P.: study conception and design, data analysis and interpretation, manuscript editing, and final manuscript approval.

Disclosure of Potential Conflicts of Interest

The authors indicate no potential conflicts of interest.

References

1 Pittenger MF, Mackay AM, Beck SC et al. Multilineage potential of adult human mesenchymal stem cells. Science 1999;284:143-147.
2 Ren G, Zhang L, Zhao X et al. Mesenchymal stem cell-mediated immunosuppression occurs via concerted action of chemokines and nitric oxide. Cell Stem Cell 2008;2:141-150.
3 Ménard C, Pacelli L, Bassi G et al. Clinical-grade mesenchymal stromal cells produced under various good manufacturing practice processes differ in their immunomodulatory properties: Standardization of immune quality controls. Stem Cells Dev 2013; 22:1789-1801.
4 Wang Y, Chen X, Cao W et al. Plasticity of mesenchymal stem cells in immunomodulation: Pathological and therapeutic implications. Nat Immunol 2014;15:1009-1016.
5 Tarte K, Gaillard J, Lataillade J-J et al. Clinical-grade production of human mesenchymal stromal cells: Occurrence of aneuploidy without transformation. Blood 2010; 115:1549-1553.
6 Sensebé L, Bourin P, Tarte K. Good manufacturing practices production of mesenchymal stem/stromal cells. Hum Gene Ther 2011;22:19-26.
7 Chen Q, Fischer A, Reagan JD et al. Oxidative DNA damage and senescence of human diploid fibroblast cells. Proc Natl Acad Sci USA 1995;92:4337-4341.
8 Wang Y, Zhang Z, Chi Y et al. Long-term cultured mesenchymal stem cells frequently develop genomic mutations but do not undergo malignant transformation. Cell Death Dis 2013;4:e950.
9 Estrada JC, Torres Y, Benguría A et al. Human mesenchymal stem cell-replicative senescence and oxidative stress are closely linked to aneuploidy. Cell Death Dis 2013;4: e691.
10 Li X-Y, Ding J, Zheng Z-H et al. Long-term culture in vitro impairs the immunosuppressive activity of mesenchymal stem cells on T cells. Mol Med Report 2012;6: 1183-1189.
11 Harding SM, Coackley C, Bristow RG. ATM-dependent phosphorylation of 53BP1 in response to genomic stress in oxic and hypoxic cells. Radiother Oncol 2011;99:307-312.
12 Schuler N, Rübe CE. Accumulation of DNA damage-induced chromatin alterations in tissue-specific stem cells: The driving force of aging? PLoS One 2013;8:e63932.
13 Tang J, Cho NW, Cui G et al. Acetylation limits 53BP1 association with damaged chromatin to promote homologous recombination. Nat Struct Mol Biol 2013;20:317-325
14 Jin Y, Kato T, Furu M et al. Mesenchymal stem cells cultured under hypoxia escape from senescence via down-regulation of p16 and extracellular signal regulated kinase. Biochem Biophys Res Commun 2010;391:1471-1476.
15 Tsai C-C, Chen Y-J, Yew T-L et al. Hypoxia inhibits senescence and maintains mesenchymal stem cell properties through down-regulation of E2A-p21 by HIF-TWIST. Blood 2011;117:459-469.
16 Li T-S, Marbán E. Physiological levels of reactive oxygen species are required to maintain genomic stability in stem cells. Stem Cells 2010;28:1178-1185.
17 Sugrue T, Lowndes NF, Ceredig R. Hypoxia enhances the radio-resistance of mouse mesenchymal stromal cells. Stem Cells 2014;32:2188-2200.
18 Bindra RS, Schaffer PJ, Meng A et al. Alterations in DNA repair gene expression under hypoxia: Elucidating the mechanisms of hypoxia-induced genetic instability. Ann N Y Acad Sci 2005;1059:184-195.
19 Bindra RS, Glazer PM. Repression of RAD51 gene expression by E2F4/p130 complexes in hypoxia. Oncogene 2007;26:2048-2057.
20 Rodríguez-Jiménez FJ, Moreno-Manzano V, Lucas-Dominguez R et al. Hypoxia causes downregulation of mismatch repair system and genomic instability in stem cells. Stem Cells 2008;26:2052-2062.
21 Bigot N, Guérillon C, Loisel S et al. ING1b negatively regulates HIF1α protein levels in adipose-derived stromal cells by a SUMOylation-dependent mechanism. Cell Death Dis 2015;6:e1612.
22 Ikura T, Tashiro S, Kakino A et al. DNA damage-dependent acetylation and ubiquitination of H2AX enhances chromatin dynamics. Mol Cell Biol 2007;27:7028-7040.
23 Zimmermann M, de Lange T. 53BP1: Pro choice in DNA repair. Trends Cell Biol 2014; 24:108-117.

24 Bonab MM, Alimoghaddam K, Talebian F et al. Aging of mesenchymal stem cell in vitro. BMC Cell Biol 2006;7:14.
25 Grayson WL, Zhao F, Bunnell B et al. Hypoxia enhances proliferation and tissue formation of human mesenchymal stem cells. Biochem Biophys Res Commun 2007;358: 948-953.
26 Chacko SM, Ahmed S, Selvendiran K et al. Hypoxic preconditioning induces the expression of prosurvival and proangiogenic markers in mesenchymal stem cells. Am J Physiol Cell Physiol 2010;299:C1562-C1570.
27 Oliver L, Hue E, Séry Q et al. Differentiation related response to DNA breaks in human mesenchymal stem cells. Stem Cells 2013;31:800-807.
28 Torsvik A, Røsland GV, Svendsen A et al. Spontaneous malignant transformation of human mesenchymal stem cells reflects cross-contamination: Putting the research field on track—Letter. Cancer Res 2010;70: 6393-6396.
29 Oliveira PH, Boura JS, Abecasis MM et al. Impact of hypoxia and long-term cultivation on the genomic stability and mitochondrial performance of ex vivo expanded human stem/stromal cells. Stem Cell Res 2012;9:225-236.
30 Nunes-Alves C. Viral infection: Manipulation of DNA repair pathways. Nat Rev Microbiol 2014;12:530-530.
31 Doucet C, Ernou I, Zhang Y et al. Platelet lysates promote mesenchymal stem cell expansion: A safety substitute for animal serum in cell-based therapy applications. J Cell Physiol 2005;205:228-236.
32 Bura A, Planat-Benard V, Bourin P et al. Phase I trial: The use of autologous cultured adipose-derived stroma/stem cells to treat patients with non-revascularizable critical limb ischemia. Cytotherapy 2014;16:245-257.
33 Kumareswaran R, Ludkovski O, Meng A et al. Chronic hypoxia compromises repair of DNA double-strand breaks to drive genetic instability. J Cell Sci 2012;125:189-199.
34 Bencokova Z, Kaufmann MR, Pires IM et al. ATM activation and signaling under hypoxic conditions. Mol Cell Biol 2009;29: 526-537.
35 Doil C, Mailand N, Bekker-Jensen S et al. RNF168 binds and amplifies ubiquitin conjugates on damaged chromosomes to allow accumulation of repair proteins. Cell 2009; 136:435-446.
36 Mallette FA, Mattiroli F, Cui G et al. RNF8- and RNF168-dependent degradation of KDM4A/JMJD2A triggers 53BP1 recruitment to DNA damage sites. EMBO J 2012;31:1865-1878.
37 Perez-Oliva AB, Lachaud C, Szyniarowski P et al. USP45 deubiquitylase controls ERCC1-XPF endonuclease-mediated DNA damage responses. EMBO J 2015;34:326-343.
38 Sharma N, Zhu Q, Wani G et al. USP3 counteracts RNF168 via deubiquitinating H2A and γH2AX at lysine 13 and 15. Cell Cycle 2013;13:106-114.
39 Gudjonsson T, Altmeyer M, Savic V et al. TRIP12 and UBR5 suppress spreading of chromatin ubiquitylation at damaged chromosomes. Cell 2012;150:697-709.
40 Stiff T, O'Driscoll M, Rief N et al. ATM and DNA-PK function redundantly to phosphorylate H2AX after exposure to ionizing radiation. Cancer Res 2004;64:2390-2396.
41 Bouquet F, Ousset M, Biard D et al. A DNA-dependent stress response involving DNA-PK occurs in hypoxic cells and contributes to cellular adaptation to hypoxia. J Cell Sci 2011;124:1943-1951.
42 Harding SM, Bristow RG. Discordance between phosphorylation and recruitment of 53BP1 in response to DNA double-strand breaks. Cell Cycle 2012;11:1432-1444.
43 Galanty Y, Belotserkovskaya R, Coates J et al. Mammalian SUMO E3-ligases PIAS1 and PIAS4 promote responses to DNA double-strand breaks. Nature 2009;462:935-939.
44 Huyen Y, Zgheib O, Ditullio RA et al. Methylated lysine 79 of histone H3 targets 53BP1 to DNA double-strand breaks. Nature 2004;432:406-411.
45 Meng AX, Jalali F, Cuddihy A et al. Hypoxia down-regulates DNA double strand break repair gene expression in prostate cancer cells. Radiother Oncol 2005;76:168-176.
46 Bindra RS, Gibson SL, Meng A et al. Hypoxia-induced down-regulation of BRCA1 expression by E2Fs. Cancer Res 2005;65: 11597-11604.
47 Koshiji M, To KK-W, Hammer S et al. HIF-1alpha induces genetic instability by transcriptionally downregulating MutSalpha expression. Mol Cell 2005;17:793-803.
48 Santos Dos F, Andrade PZ, Boura JS et al. Ex vivo expansion of human mesenchymal stem cells: A more effective cell proliferation kinetics and metabolism under hypoxia. J Cell Physiol 2010;223:27-35.
49 Zheng W, Khrapko K, Coller HA et al. Origins of human mitochondrial point mutations as DNA polymerase gamma-mediated errors. Mutat Res 2006;599:11-20.
50 Alison MR, McDonald SAC, Lin WR et al. Protection of mitochondrial genome integrity: A new stem cell property? Hepatology 2010;51:354-354.
51 Cho YM, Kim JH, Kim M et al. Mesenchymal stem cells transfer mitochondria to the cells with virtually no mitochondrial function but not with pathogenic mtDNA mutations. PLoS One 2012;7:e32778.
52 Baines HL, Turnbull DM, Greaves LC. Human stem cell aging: Do mitochondrial DNA mutations have a causal role? Aging Cell 2014;13:201-205.


See www.StemCells.com for supporting information available online.